Micro Magnetometer Calibration for Accurate Orientation Estimation

Zhi-Qiang Zhang and Guang-Zhong Yang, *Fellow, IEEE*

Abstract—Micro-magnetometers, together with inertial sensors, are widely used for attitude estimation for a wide variety of applications. However, appropriate sensor calibration, which is essential to the accuracy of attitude reconstruction, must be performed in advance. Thus far, many different magnetometer calibration methods have been proposed to compensate for errors such as scale, offset, and nonorthogonality. They have also been used for obviate magnetic errors due to soft and hard iron. However, in order to combine the magnetometer with inertial sensor for attitude reconstruction, alignment difference between the magnetometer and the axes of the inertial sensor must be determined as well. This paper proposes a practical means of sensor error correction by simultaneous consideration of sensor errors, magnetic errors and alignment difference. We take the summation of the offset and hard iron error as the combined bias, and then amalgamate the alignment difference and all the other errors as a transformation matrix. A two-step approach is presented to determine the combined bias and transformation matrix separately. In the first step, the combined bias is determined by finding a optimal ellipsoid that can best fit the sensor readings. In the second step, the intrinsic relationships of the raw sensor readings are explored to estimate the transformation matrix as a homogeneous linear least squares problem. Singular value decomposition is then applied to estimate both the transformation matrix and magnetic vector. The proposed method is then applied to calibrate our sensor node. Although there is no ground-truth for the combined bias and transformation matrix for our node, the consistency of calibration results among different trials and less than $3°$ root mean square error (RMSE) for orientation estimation have been achieved, which illustrates the effectiveness of the proposed sensor calibration method for practical applications.

Index Terms—Magnetometer, Calibration, System Identification, Ellipsoid fitting, Homogeneous linear least-squares

I. INTRODUCTION

In conjunction with inertial sensors, micro-magnetometers have been widely used to determine attitude information, which can be applied for a variety of applications, from delivering realistic animation in filming and entertainment to assessing the performance of professional athletes [1] [2]. Clinically, it can also be used to analyse the biomechanics of patients. The analysis provides an objective measure of physical function to aid interventional planning, evaluate the outcomes of surgical procedures, which are exceptionally beneficial for many biomedical applications, such as rehabilitation [3] [4], fall detection [5] [6] and gait analysis [7] [8]. Thus far, extensive research has been performed in order to accurately estimate attitude information from micro inertial and magnetic sensor measurements [9] [10]. In practice, the achievable accuracy of attitude estimation is highly dependent on the quality of the sensor measurements. Therefore, appropriate sensor calibration, as the important prerequisite step for attitude estimation, must be performed in advance to compensate for errors in sensor readings.

Recently, many magnetometer calibration methods have been proposed to compensate for sensor errors (such as scale factor, offset, nonorthogonality) and magnetic errors (soft and hard iron) [11] [12]. For instance, Gambhir [13] proposed to use centering approximation to formulate the bias calibration problem in the linear least-squares form. Alonso et al. [14] [15] further improved Gambhir's approach in terms of robustness and efficiency. These two methods are easy to implement in practice, but they only consider the bias error with all the other error sources ignored. In recent papers, more advanced magnetometer calibration algorithms have been proposed. They not only consider the bias error but also tackle sensitivity, nonorthogonality and magnetic errors in the sensor space. For example, both Elkaim et al. [16] and Gebre-Egziabher et al. [17] have formulated the calibration problem in a pseudo-linear least-squares form. Batch linearized least-squares algorithms were derived to obtain the calibration parameters including non-orthogonality, magnetic, sensitivity and bias. Renaudin et al. [18] proposed a complete model to compensate for sensor and magnetic errors. An adaptive least-squares estimator, which provided a consistent solution to the ellipsoid fitting problem has been derived. Based on the similar sensor error model, Vasconcelos et al. [19] proposed an iterative Maximum Likelihood Estimator (MLE) which allowed for the formulation of the calibration problem as an optimization process in terms of the likelihood of sensor readings. Such method, however, is influenced by the initial approximation, which may make the MLE converge to a local maximum. To overcome this drawback, Wu et al. [20] proposed to use a particle swarm optimization (PSO) strategy combined with a stretching technique, which could help to eliminate the local maxima. Springmann et al. [21] and Pang et al [22] presented similar work for magnetometer calibration. However, all the aforementioned calibration methods only considered the magnetometer calibration in its sensor frame. In order to integrate the magnetometer with inertial sensor for attitude estimation, the alignment difference between the magnetometer and the inertial sensor axes should also be

considered during the calibration process.

In fact, there are also several studies estimating the alignment difference by simultaneous calibration of inertial and magnetic sensors. For instance, Bonnet et al. [11] proposed to estimate the difference by finding three vectors in magnetometer sensor frame and their corresponding vectors in the reference inertial frame, but it is difficult to find such vectors in practice. Kow et al [12] derived an easy-to-use calibration algorithm that could be used to calibrate a combination of a magnetometer and inertial sensors. They made use of probabilistic models and obtained the calibration algorithm as the solution to a maximum likelihood problem. In [23], they further extended this work and proposed to use grey-box system identification approach to simplify the computation of the maximum likelihood estimates. The method can be used to estimate the alignment difference between the axes of the magnetometer and the inertial sensor, albeit being complex to implement in practice. In our previous study [24], similar work has been conducted but we ignored such alignment difference in our calibration process.

The motivation of the paper is to further extend our previous paper in [24] and tackle the sensor errors, magnetic errors and also the alignment difference between the axes of the magnetometer and the inertial sensor. With the proposed approach, we take the summation of the offset and hard iron error as the combined bias, and then amalgamate the alignment difference and all the other errors as a transformation matrix. A two-step approach is adopted to determine the combined bias and transformation matrix separately. In the first step, the combined bias is determined by finding the optimal ellipsoid that can best fit the sensor readings. Subsequently, the intrinsic relationships of the sensor readings are explored to determine the transformation matrix by using a homogeneous linear least-squares method. Singular value decomposition is used to estimate both the transformation matrix and magnetic vector. The rest of the paper is organized as follows. Section II presents the proposed approach for micro magnetometers calibration, including the sensor error model, combined bias estimation and transformation matrix determination. Detailed simulation and experimental results are described in Section III and the conclusion derived from the studies is presented in Section IV.

II. OUR METHOD

A. Sensor error model

For the description of micro-magnetometers, all sensor readings should be first converted to physical quantities in metric units. To this end, there are mainly three types of errors that need to be distinguished: sensor errors, magnetic errors and alignment difference between the axes of the magnetometer and the inertial sensor.

1) Sensor errors: A triaxial sensor has three sensitivity axes x, y and z, spanning a three dimensional space. Ideally, the sensor sensitivity axes should be orthogonal to each other, but due to inevitable imperfection during the fabrication process, this is not guaranteed. Therefore, orthogonalization of the axes is necessary. Denote T as the Gram-Schmidt orthogonalization

matrix, so T can be written as:

$$T = \begin{bmatrix} 1 & 0 & 0 \\ \alpha & 1 & 0 \\ \beta & \gamma & 1 \end{bmatrix}. \quad (1)$$

The offset of the sensor readings is modelled as a constant bias vector $b = [b_x, \ b_y, \ b_z]^T$. The raw senor reading is directly proportional to the voltage level, which should be converted to physical quantities through a scale factor matrix S as

$$S = \begin{bmatrix} s_x & 0 & 0 \\ 0 & s_y & 0 \\ 0 & 0 & s_z \end{bmatrix} \quad (2)$$

2) Magnetic errors: In practice, the external magnetic field can introduce both hard iron and soft iron errors. The hard iron effect is due to remanence of magnetized iron materials, which is constant and can be represented by a bias vector $b_{hi} = [b_{hi}^x, \ b_{hi}^y, \ b_{hi}^z]^T$. Soft iron errors are generated by the interaction of the external magnetic field with the ferromagnetic materials in the vicinity of the sensor. This changes the intensity, as well as the direction of the sensed magnetic field. The soft iron effect is usually modelled by a 3×3 matrix

$$A_{si} = \begin{bmatrix} a_{si}^{11} & a_{si}^{12} & a_{si}^{13} \\ a_{si}^{21} & a_{si}^{22} & a_{si}^{23} \\ a_{si}^{31} & a_{si}^{32} & a_{si}^{33} \end{bmatrix}. \quad (3)$$

3) Alignment difference: For orientation estimation, the magnetometer is usually mounted together with the inertial sensors. The geometrical relationship of the axes of different sensors' orthogonal sensitivity is important, especially with respect to the overall system accuracy. In practice, the orthogonal sensitivity axes are aligned to the inertial coordinate through a rotation matrix R as:

$$R = R_z(\psi) R_y(\theta) R_x(\phi) \quad (4)$$

where

$$R_x(\phi) = \begin{bmatrix} 1 & 0 & 0 \\ 0 & cos(\phi) & -sin(\phi) \\ 0 & sin(\phi) & cos(\phi) \end{bmatrix}, \quad (5)$$

$$R_y(\theta) = \begin{bmatrix} cos(\theta) & 0 & sin(\theta) \\ 0 & 1 & 0 \\ -sin(\theta) & 0 & cos(\theta) \end{bmatrix} \quad (6)$$

and

$$R_z(\psi) = \begin{bmatrix} cos(\psi) & -sin(\psi) & 0 \\ sin(\psi) & cos(\psi) & 0 \\ 0 & 0 & 1 \end{bmatrix}. \quad (7)$$

4) Error Parameterization: After combing the sensor errors, magnetic errors and alignment difference, the three-axis magnetometer measurement can be represented by using the following error model [12] [18]:

$$u = RTSA_{si}(g - b - b_{hi}), \quad (8)$$

where u is the measured physical quantities in metric unit in the inertial coordinate, and the g is sensor voltage readings in the non-orthogonal magnetometer coordinate frame.

The purpose of sensor calibration is to estimate the value of the parameter vector

$$\zeta = \left[\alpha, \beta, \gamma, \phi, \psi, \theta, s_x, s_y, s_z, b_x, b_y, b_z, b_{hi}^x, b_{hi}^y, b_{hi}^z, a_{si}^{11}, \cdots, a_{si}^{33}\right]^T$$

given J sensor raw readings g_j, where $j = 1, 2, \cdots, J$ and the magnitude of the local magnetic field M. The estimation of ζ can be written as:

$$\hat{\zeta} = \underset{\zeta}{\operatorname{argmin}}\{L(\zeta)\} \tag{9}$$

subject to

$$|u_j| = M \tag{10}$$

where

$$L(\zeta) = \sum_{j=1}^{J} \left\| u_j - RTSA_{si}(g_j - b - b_{hi}) \right\|^2 \tag{11}$$

u_j is the measured physical quantity for the sensor reading g_j, $|\cdot|$ and $\|\cdot\|$ are the magnitude and Frobenius norm operators, respectively. Here, j is the index of different orientation or rotation that the sensor node is set to. In (10), we implicitly assume that all the magnetic distortion and local magnetic field are constant. This is a reasonable assumption as long as the sensor node is placed at the same position in different orientations during the calibration process.

In practice, it is difficult to find a globally optimized solution for ζ due to the difficulty of acquiring u_j. Since the main purpose of the sensor calibration is to find an accurate u for any sensor reading g, there is no need to estimate the 24 parameters individually. Therefore, we propose a two-step parameter estimation scheme to simplify the optimization process, i.e., 1) estimate the combined bias $B = b + b_{hi}$ 2) estimate the transformation matrix $H = RTSA_{si}$. The advantage of combining the different parameters together is not only to reduce the unknown parameters from 24 to 12, but also to take the other unmodelled linear time invariant errors and distortions into account.

B. Combined bias estimation

After defining the combined bias B and the transformation matrix H, the new sensor error model can be written as

$$u = H(g - B). \tag{12}$$

For any sensor reading g_j, we can have

$$|H \cdot (g_j - B)| = M. \tag{13}$$

By expanding the above equation, we can get:

$$(g_j - B)^T \cdot (H)^T \cdot H \cdot (g_j - B) = M^2. \tag{14}$$

Thus we can normalize the above equation as:

$$(g_j - B)^T \cdot \left(\frac{H}{M}\right)^T \cdot \frac{H}{M} \cdot (g_j - B) = 1. \tag{15}$$

Expanding this equation we obtain

$$(g_j)^T \cdot \Sigma \cdot g_j - (g_j)^T \cdot \Gamma + \Upsilon = 0 \tag{16}$$

where

$$\Sigma = \left(\frac{H}{M}\right)^T \frac{H}{M}$$
$$\Gamma = 2\Sigma \cdot B \tag{17}$$
$$\Upsilon = (B)^T \cdot \Sigma \cdot B - 1$$

This equation is the algebraic equation of an ellipsoid [19] [24], and the calibration problem now becomes finding an arbitrarily oriented ellipsoid which fits the J points $g_1, g_2 \cdots g_J$ best. There is abundant literature addressing this problem [25] [26] [27]. For this study, the least squares ellipsoid fitting method proposed in [27] is used, and the value of Σ, Γ and Υ can be then obtained. Denote the estimates for Σ and Γ as $\hat{\Sigma}$, $\hat{\Gamma}$, we can then have the following properties for H and B:

$$(H)^T \cdot H = M^2\hat{\Sigma}$$
$$B = \frac{1}{2}\left(\hat{\Sigma}\right)^{-1}\hat{\Gamma}. \tag{18}$$

Since $\hat{\Sigma}$ is a positive definite matrix, an eigen-decomposition can be applied:

$$\hat{\Sigma} = \Lambda D \Lambda^T \tag{19}$$

where Λ corresponds to the eigenvectors of $\hat{\Sigma}$, and D is the diagonal matrix containing the eigenvalues, so we can define another matrix K as

$$K = M\Lambda\sqrt{D}\Lambda^T \tag{20}$$

satisfying

$$K^T K = M\Lambda\sqrt{D}\Lambda^T M S \sqrt{D}\Lambda^T$$
$$= M^2 \Lambda D \Lambda^T \tag{21}$$
$$= M^2 \hat{\Sigma}.$$

However, given any rotational matrix Ω, we can also have

$$(\Omega K)^T \Omega K = M S \sqrt{D}\Lambda^T \Omega^T \Omega M \Lambda \sqrt{D}\Lambda^T$$
$$= M^2 \Lambda D \Lambda^T \tag{22}$$
$$= M^2 \hat{\Sigma}.$$

Therefore, the factorization $(H)^T H = M^2 \hat{\Sigma}$ is not unique, and H can be any matrix in the form of ΩK, so it is impossible to acquire the exact transformation matrix H through the ellipsoid fitting, while the combined bias B can be estimated accurately. In the next section, we will discuss how to determine the transformation matrix by exploring the intrinsic relationships among the sensor readings.

C. Estimation of transformation matrix

In the previous section, any two sensor readings g_i and $g_j (i = 1, 2 \cdots J$ and $i \neq j)$ are used independently. However, both indexes i and j indicate the orientations or rotations that the sensor node is set to; therefore, we can also get the rotation difference R_j^i between the ith orientation and j^{th} orientation. Therefore, we have:

$$u_i = H \cdot (g_i - B) \tag{23}$$

and

$$u_j = H \cdot (g_j - B) \tag{24}$$

where $u_j = R_j^i u_i$. Then $u_j - u_i$ can be written as

$$u_j - u_i = \left(R_j^i - I_3\right) u_i = H(g_j - g_i) \quad (25)$$

where I_3 is the 3×3 identity matrix. The above equation can then be expanded as:

$$\begin{cases} \left(R_j^i - I_3\right) u_i^x - (g_j - g_i)H_1^T = 0 \\ \left(R_j^i - I_3\right) u_i^y - (g_j - g_i)H_2^T = 0 \\ \left(R_j^i - I_3\right) u_i^z - (g_j - g_i)H_3^T = 0 \end{cases} \quad (26)$$

where

$$H = \begin{bmatrix} H_1 \\ H_2 \\ H_3 \end{bmatrix}$$

and $u_i = [u_i^x, u_i^y, u_i^z]$. Define

$$A_j^i = \left[R_j^i - I_3, \ \Delta_j^i\right]^T \quad (27)$$

and

$$X = \left[u_i^T \ H_1 \ H_2 \ H_3\right]^T \quad (28)$$

we can have the matrix representation for (26):

$$A_j^i X = 0 \quad (29)$$

where

$$\Delta_j^i = \begin{bmatrix} -(g_j - g_i)^T & 0 & 0 \\ 0 & -(g_j - g_i)^T & 0 \\ 0 & 0 & -(g_j - g_i)^T \end{bmatrix}.$$

However, it is necessary to have at least 12 equations to find the non-zero solution for X. Since any pair of g_i and g_j leads to three equations as shown in (26), at least 5 sensor readings are required. Given $J >> 5$ in the calibration process, we can define

$$A = \begin{bmatrix} A_1^i \\ \vdots \\ A_{i-1}^i \\ A_{i+1}^i \\ \vdots \\ A_J^i \end{bmatrix}$$

and we can then derive the following homogeneous linear least-squares problem:

$$AX = 0 \qquad \textit{subject to } X \neq 0. \quad (30)$$

The vector X can be recovered from the singularity value decomposition (SVD) related techniques [28] [29]. The SVD of the matrix A is calculated as:

$$A = U\Sigma V^T \quad (31)$$

where the columns of U contain the eigenvectors of AA^T, the columns of V contain the eigenvectors of $A^T A$, and the diagonal of Σ indicates the singular values of A. The last column of matrix V corresponding to the smallest singular value of A, is taken as the non-zero solution of the vector X. However, if the last column vector v_X is the solution for $AX = 0$, then κv_X, where κ is a arbitrary scale, will also be a solution; therefore, the next step is to determine the value of κ. According to the definition of vector X in (28), the vector

κv_X can be easily reshaped into the magnetic vector κv_X^u and the transformation matrix κv_X^H. Since the magnitude of the local magnetic field is M, we can then have

$$\kappa^2 \|v_X^u\| = M^2 \quad (32)$$

so κ can be calculated as:

$$\kappa = \pm\sqrt{\frac{M^2}{\|v_X^u\|}}. \quad (33)$$

Since the sign of κ will not affect the performance of a magnetometer for orientation estimation in practice, we always chose the positive κ in our implementation.

III. SIMULATION AND EXPERIMENTAL RESULTS

In order to evaluate the performance of the proposed magnetometer calibration method, detailed simulation and laboratory experiments were conducted. The simulation study was based on Monte Carlo simulation to illustrate the performance of the proposed calibration method. For the experimental results presented in this paper, we used the Body Sensor Network (BSN) platform [30] [31] developed by our lab, which consists of three stackable daughter boards: the sensor board, the main processor board, and the battery board. They are connected via a stackable connector design as shown in Fig. 1(a). Each BSN node is equipped with an Analog Devices ADXL330 (8 bits ADC used) [32] for 3D acceleration measurement, an InvenSense ITG-3200 digital gyroscope (12 bits ADC used) [33] for 3D angular velocity measurement, and a Honeywell HMC5843 (12 bits ADC used) [34] for 3D magnetic field measurement. In order to calibrate the BSN node, a bespoke housing for the BSN node is designed as shown in Fig. 1(b).
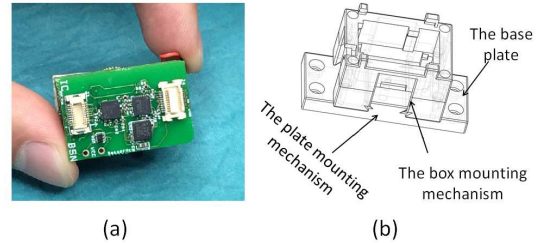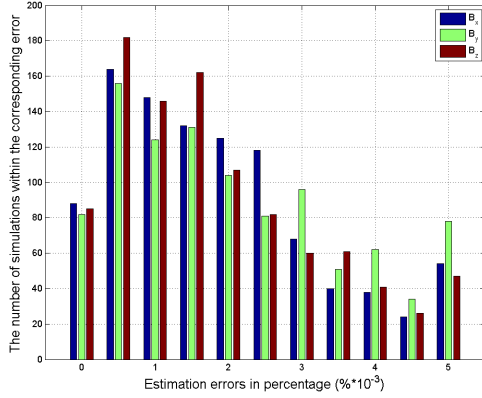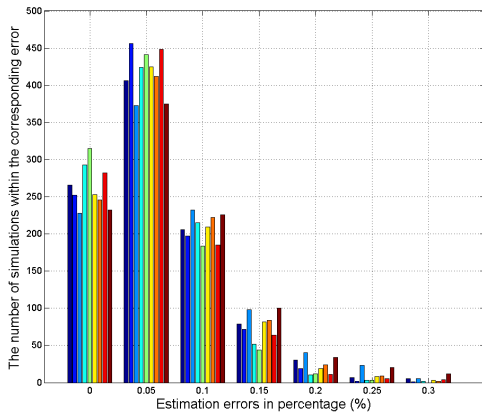

(a)   (b)

Figure 1. The BSN hardware platform used for this study. (a) BSN Sensor Node and its stackable sensor daughter boards. (b) The bespoke housing for the BSN Sensor Node.

Table I
MODEL PARAMETERS USED FOR MAGNETOMETER CALIBRATION

Nonorthogonality	$\alpha = 0.1$	$\beta = 0.1$	$\gamma = 0.1$
Mounting	$\phi = 0.1$	$\theta = 0.1$	$\psi = 0.1$
Scaling (mg)	$s_x = 1/1.2$	$s_y = 1/1.383$	$s_z = 1/1.12$
Bias	$b_x = 32000$	$b_y = 32000$	$b_z = 32000$
Hard Iron	$b_{hi}^x = 268$	$b_{hi}^y = -123$	$b_{hi}^z = -109$
Soft Iron	$a_{si}^{11} = 1$ $a_{si}^{21} = 0.1$ $a_{si}^{31} = 0.1$	$a_{si}^{12} = 0.1$ $a_{si}^{22} = 1$ $a_{si}^{32} = 0.1$	$a_{si}^{13} = 0.1$ $a_{si}^{32} = 0.1$ $a_{si}^{33} = 1$

(a) Combined bias

(b) Transformation Matrix

(c) Magnetic vector

Figure 2. Statistical results for combined bias B, transformation matrix H and magnetic vector u_i over the 1000 simulations, demonstrating the small estimation errors involved.

A. Sensor Calibration Simulation Results

In the simulation experiment, we evaluated the estimation results of the magnetometer sensor model parameters when we randomly position the sensor in 30 different orientations. A zero mean Gaussian distributed error with variance 0.1 mg

was added to the voltage readings y to simulate sensor noise. In Table I, the settings used in the simulation are summarized.
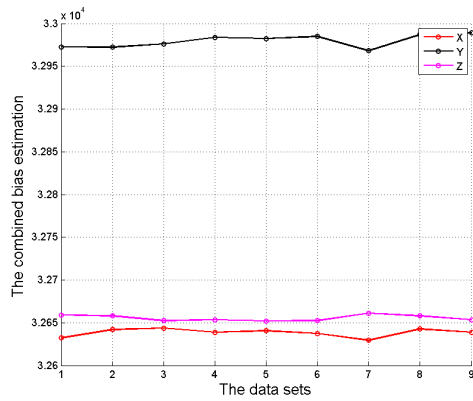
The simulation was repeated for 1000 times, and statistical results for B and H are given in Fig 2. As we can see from Fig 2(a), over 92% of the estimated combined bias has smaller error than 0.005%. It can also be noted that the maximum estimation error for the combined bias is 0.012%, which is small and imperceptible. Fig 2(b) shows the error histogram for the nine elements of the transformation matrix. It is evident that the majority of the estimated errors are located between 0 and 0.15%. Although the transformation matrix estimation error has a slight increase over that of the combined bias estimation, it is still very small and negligible. The SVD described in section II.C can not only estimate the transformation matrix, but also provide the reference magnetic vector, which is given in the Fig. 2(c). Similarly, the errors of the estimated magnetic vector are also small (0.05%). In conclusion, the above analysis has shown that the proposed ellipsoid fitting method can estimate the combined bias values accurately. By exploring the relationships among raw sensor readings, it is also possible to determine the transformation matrix without the need of extra devices to measure the magnetic information in advance.
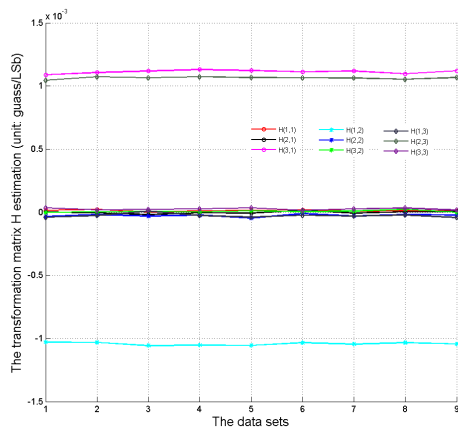
B. Calibration Results

We then applied the proposed magnetometer calibration method to our BSN node. The sensor node was rotated to different orientations to evaluate the reproducibility of the proposed method. To make sure the magnetic distortion and local magnetic field are constant for different orientations, the sensor node was kept in a small area with ignorable translational movement when rotating the sensor node. Nine data sets have been acquired with a sampling frequency of 33 Hz. In each data set, the sensor node was randomly placed at 20-30 different orientations, and at least 5s of data were collected for each orientation. Instead of using all the raw sensor readings for each orientation, only the mean value of these readings was used to increase the signal-to-noise ratio (SNR) for sensor model parameter determination. Since the proposed method involves many matrix operations, all the data was sent back to a PC with 3.40 GHz Intel Core i5 processor and 8G RAM for processing. Once the transformation matrix H and combined bias B are determined, we can then set the values of H and B permanently for each BSN node.

The combined bias and the transformation matrix estimation results obtained from these nine independent data sets are shown in Fig. 3(a) and Fig. 3(b). As we can see from the figures, both the combined bias and transformation matrix estimation results are similar for all the trials performed, and the deviations are small compared to the mean values. The consistency among all the nine trials indicates the good repeatability of the proposed method. It is also worth nothing that although there is no ground-truth for the combined bias and transformation matrix, the consistency of the data illustrates the robustness of our proposed method.

The main purpose of the magnetometer calibration is to accurately convert the raw sensor readings into physical quantities in metric unit, we therefore randomly chose 20 raw
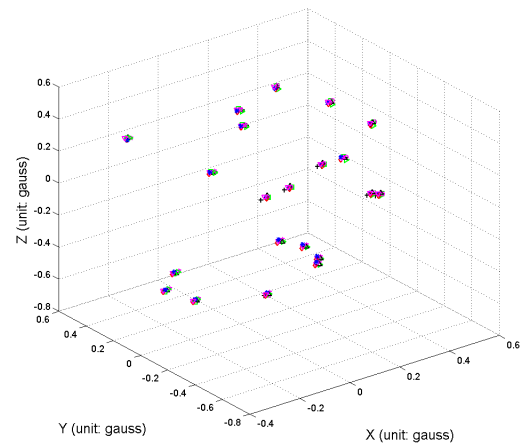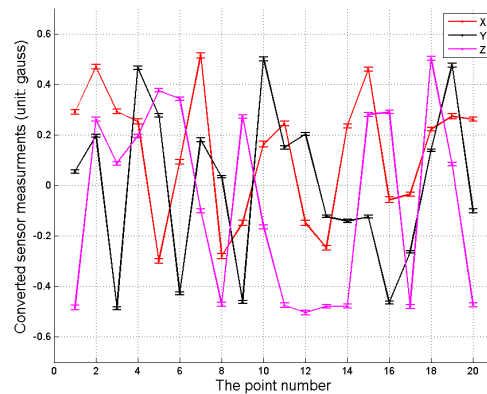
(a) Combined bias

(b) Transformation Matrix

Figure 3. The calibration results for the BSN sensor node. During the experiments, the same calibration method was repeated 9 times on the same sensor node. Although there is no ground-truth for the combined bias and transformation matrix, the estimation results have shown good consistency, which illustrates the robustness of our proposed method.

(a) The converted sensor measurements in gauss

(b) Mean and standard deviation

Figure 4. The conversion of the 20 randomly chosen raw sensor readings into the metric unit (gauss) using the 9 sets of estimated combined bias and transformation matrix. Small deviations were achieved for all the data points using the 9 sets of the conversion parameters.

sensor readings and then converted them into meaningful quantities in gauss in our second experiment. Fig. 4(a) shows the converted sensor measurements using the 9 sets of the estimated combined bias and the transformation matrix. It is evident that for any sensor readings, all the nine conversions are close to each other, which again illustrates the effectiveness and robustness of the proposed calibration method. The quantitative results for these conversions are provided in the Fig. 4(b). In the figure, the mean and the standard deviation of the 9 conversions for each raw sensor reading are provided. The maximum standard deviation is less than 0.01, resulting the variance smaller than 0.0001 [35]. However, for orientation estimation, the variance for the magnetometer measurement is normally set to be larger than 0.01. This means that the small variations of the different conversions can be taken as the measurement noise, which can be well modeled by the measurement covariance matrix in the orientation estimation applications.
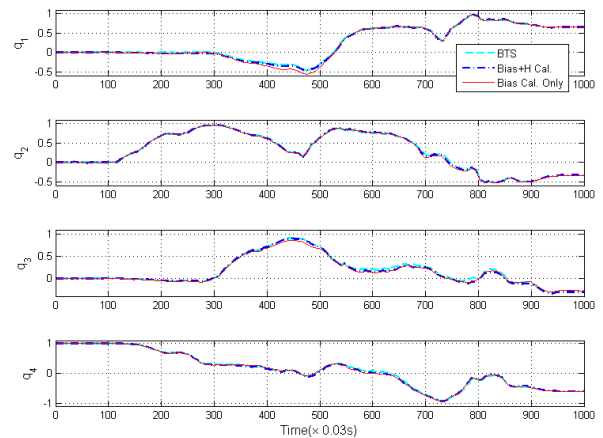

Figure 5. The orientation estimation results in quaternion compared to the BTS measurements after the magnetometer calibration.

Table II
THE RMS, MEAN, SD AND CORRELATION COEFFICIENTS OF THE
ESTIMATED ATTITUDE COMPARED TO THE BTS OPTICAL SYSTEM.

	H+B Calibration		B Calibration only	
	RMS (unit: rad) (Mean,SD)	Correlation Coefficient	RMS (unit: rad) (Mean,SD)	Correlation Coefficient
Roll	0.0397 (0.0014± 0.0397)	0.9970	0.0548 (-0.0252±0.0487)	0.9763
Pitch	0.0698 (-0.0431±0.0549)	0.9930	0.0854 (-0.0171±0.0836)	0.9720
Yaw	0.0507 (0.0060±0.0503)	0.9981	0.0744 (0.0095±0.0738)	0.9873

C. Attitude estimation using calibrated sensors

As mentioned earlier, the magnetometer and the inertial sensors are widely used for attitude estimation in biomedical applications. Since the magnetometer is calibrated and aligned to the inertial sensor axes, we then used these three sensors together for biomotion analysis. In our experiment, the sensor node was placed on a human forearm to track its movement. The subject then rotated the arm arbitrarily and smoothly to make sure there is no linear acceleration interference or magnetic disturbance. We then used algorithm presented in [36] to determine the orientation of the arm. Fig. 5 shows the estimated orientation using the proposed method, and the ground-truth measurements from the optical motion tracking system BTS SMART-D [37] are also shown in the figure. It is evident that there is significant improvement after taking the transformation matrix into consideration. Since the gyroscope integration drift cannot be compensated if only the combined bias was considered; therefore, there were some errors in the estimated attitude if the transformation matrix was ignored. The quantitative comparison results between the BTS system and BSN sensor platform are shown in Table II. From the results derived, it is evident that the proposed method significantly reduces the root mean square (RMS) errors. There is also an excellent correlation between the calibrated result with that of the BTS system.

The above analyses have shown that the proposed magnetometer calibration method can significantly improve the attitude estimation accuracy for bio-motion analysis applications. This suggests that the calibration method can recover the underlying sensor model parameters accurately. Based on the derived sensor model, the sensor readings can be converted to physical quantities in metric units for accurate attitude estimation.

IV. CONCLUSIONS

In this paper, a two-step approach has been presented to tackle all the parameters involved in the sensor errors, magnetic errors and also the alignment difference between the magnetometer and the inertial sensor axes. The summation of the offset and hard iron error was taken as a combined bias, while all the other errors were combined together as the transformation matrix. In our method, the combined bias was determined by elliptical fitting. The relationship of the raw sensor readings was then explored to extract the transformation

matrix. Singular value decomposition was then applied to estimate both the transformation matrix and the magnetic vector. Detailed validation results demonstrate the effectiveness of the proposed sensor calibration method.

It should be noted that for the current method, it does not take temperature related drift into consideration. Although this can be addressed by periodic recalibration, it may present difficulties for practical applications. Further work is therefore required for continuous self-calibration with consideration of different temporal characteristics of the sensors combined with the use of temperature controlled casing designs to minimise these errors.

REFERENCES

[1] Z.-Q. Zhang and J.-K. Wu, "A novel hierarchical information fusion method for three-dimensional upper limb motion estimation," *Instrumentation and Measurement, IEEE Transactions on*, vol. 60, no. 11, pp. 3709–3719, 2011.

[2] Z. Zhang, A. Panousopoulou, and G.-Z. Yang, "Wearable sensor integration and bio-motion capture: A practical perspective," in *Body Sensor Networks*. Springer, 2014, pp. 495–526.

[3] S. Huang, C. Luo, S. Ye, F. Liu, B. Xie, C. Wang, L. Yang, Z. Huang, and J. Wu, "Motor impairment evaluation for upper limb in stroke patients on the basis of a microsensor," *International Journal of Rehabilitation Research*, vol. 35, no. 2, pp. 161–169, 2012.

[4] B. H. Koning, M. M. van der Krogt, C. T. Baten, and B. F. Koopman, "Driving a musculoskeletal model with inertial and magnetic measurement units," *Computer methods in biomechanics and biomedical engineering*, no. ahead-of-print, pp. 1–11, 2013.

[5] W. Xu, M. Zhang, A. A. Sawchuk, and M. Sarrafzadeh, "Robust human activity and sensor location corecognition via sparse signal representation," *Biomedical Engineering, IEEE Transactions on*, vol. 59, no. 11, pp. 3169–3176, 2012.

[6] O. D. Lara and M. A. Labrador, "A survey on human activity recognition using wearable sensors," *Communications Surveys & Tutorials, IEEE*, vol. 15, no. 3, pp. 1192–1209, 2013.

[7] A. Salarian, P. R. Burkhard, F. J. Vingerhoets, B. M. Jolles, and K. Aminian, "A novel approach to reducing number of sensing units for wearable gait analysis systems," *Biomedical Engineering, IEEE Transactions on*, vol. 60, no. 1, pp. 72–77, 2013.

[8] X. Meng, Z.-Q. Zhang, J.-K. Wu, W.-C. Wong, and H. Yu, "Self-contained pedestrian tracking during normal walking using an inertial/magnetic sensor module," *Biomedical Engineering, IEEE Transactions on*, vol. 61, no. 3, pp. 892–899, March 2014.

[9] A. M. Sabatini, "Quaternion-based extended kalman filter for determining orientation by inertial and magnetic sensing," *Biomedical Engineering, IEEE Transactions on*, vol. 53, no. 7, pp. 1346–1356, 2006.

[10] Z.-Q. Zhang, L.-Y. Ji, Z.-P. Huang, and J. Wu, "Adaptive information fusion for human upper limb movement estimation," *Systems, Man and Cybernetics, Part A: Systems and Humans, IEEE Transactions on*, vol. 42, no. 5, pp. 1100–1108, 2012.

[11] S. Bonnet, C. Bassompierre, C. Godin, S. Lesecq, and A. Barraud, "Calibration methods for inertial and magnetic sensors," *Sensors and Actuators A: Physical*, vol. 156, no. 2, pp. 302–311, 2009.

[12] M. Kok, J. D. Hol, T. Schon, F. Gustafsson, and H. Luinge, "Calibration of a magnetometer in combination with inertial sensors," in *Information Fusion (FUSION), 2012 15th International Conference on*. IEEE, 2012, pp. 787–793.

[13] B. Gambhir, "Determination of magnetometer biases using module residg," *Computer Sciences Corporation, Tech. Rep*, pp. 3000–32 700, 1975.

[14] R. Alonso and M. D. Shuster, "Twostep: a fast robust algorithm for attitude-independent magnetometer-bias determination," *Journal of the Astronautical Sciences*, vol. 50, no. 4, pp. 433–452, 2002.

[15] R. Alonso and M.-D. Shuster, "Complete linear attitude-independent magnetometer calibration," *Journal of the Astronautical Sciences*, vol. 50, no. 4, pp. 477–490, 2002.

[16] G. H. Elkaim and C. C. Foster, "Metasensor: Development of a low-cost, high quality attitude heading reference system," in *Proceedings of the ION GNSS Meeting, Fort Worth, Texas*, 2006, pp. 1124–1135.

[17] D. Gebre-Egziabher, G. Elkaim, P. David, and B. Parkinson, "Calibration of strapdown magnetometers in magnetic field domain," *Journal of Aerospace Engineering*, vol. 19, no. 2, pp. 87–102, 2006.

[18] V. Renaudin, M. H. Afzal, and G. Lachapelle, "Complete triaxis magnetometer calibration in the magnetic domain," *Journal of Sensors*, vol. 2010, 2010.

[19] J. Vasconcelos, G. Elkaim, C. Silvestre, P. Oliveira, and B. Cardeira, "Geometric approach to strapdown magnetometer calibration in sensor frame," *Aerospace and Electronic Systems, IEEE Transactions on*, vol. 47, no. 2, pp. 1293–1306, 2011.

[20] Z. Wu, Y. Wu, X. Hu, and M. Wu, "Calibration of three-axis magnetometer using stretching particle swarm optimization algorithm," *Instrumentation and Measurement, IEEE Transactions on*, vol. 62, no. 2, pp. 281–292, 2013.

[21] J. C. Springmann and J. W. Cutler, "Attitude-independent magnetometer calibration with time-varying bias," *Journal of Guidance, Control, and Dynamics*, vol. 35, no. 4, pp. 1080–1088, 2012.

[22] H. Pang, Q. Zhang, W. Wang, J. Wang, J. Li, S. Luo, C. Wan, D. Chen, M. Pan, and F. Luo, "Calibration of three-axis magnetometers with differential evolution algorithm," *Journal of Magnetism and Magnetic Materials*, vol. 346, pp. 5–10, 2013.

[23] M. Kok and T. Schon, "Maximum likelihood calibration of a magnetometer using inertial sensors," in *Proceedings of the 18th World Congress of the International Federation of Automatic Control (IFAC)*, 2014.

[24] Z.-Q. Zhang and G.-Z. Yang, "Calibration of miniature inertial and magnetic sensor units for robust attitude estimation," *Instrumentation and Measurement, IEEE Transactions on*, vol. 63, no. 3, pp. 711–718, March 2014.

[25] A. Fitzgibbon, M. Pilu, and R. Fisher, "Direct least square fitting of ellipses," *Pattern Analysis and Machine Intelligence, IEEE Transactions on*, vol. 21, no. 5, pp. 476–480, 1999.

[26] I. Markovsky, A. Kukush, and S. Huffel, "Consistent least squares fitting of ellipsoids," *Numerische Mathematik*, vol. 98, no. 1, pp. 177–194, 2004.

[27] N. Chernov and H. Ma, "Least squares fitting of quadratic curves and surfaces," *Computer Vision*, pp. 285–302, 2011.

[28] A. Yeredor and B. De Moor, "On homogeneous least-squares problems and the inconsistency introduced by mis-constraining," *Computational statistics & data analysis*, vol. 47, no. 3, pp. 455–465, 2004.

[29] K. Inkilä, "Homogeneous least squares problem," *Photogrammetric Journal of Finland*, vol. 19, no. 2, 2005.

[30] Z.-Q. Zhang, J. Pansiot, B. Lo, and G.-Z. Yang, "Human back movement analysis using bsn," in *Body Sensor Networks (BSN), 2011 International Conference on*. IEEE, 2011, pp. 13–18.

[31] B. Lo and G. Yang, "Key technical challenges and current implementations of body sensor network," in *Proc. 2nd International Workshop on Body Sensor Networks (BSN 2005)*, 2005.

[32] Analog Devices ADXL330. [Online]. Available: http://www.analog.com/en/sensors/inertial-sensors/adxl330/products/product.html

[33] Invensense ITG-3200. [Online]. Available: http://invensense.com/mems/gyro/itg3200.html

[34] Honeywell HMC5483. [Online]. Available: www.magneticsensors.com/datasheets/HMC5843.pdf

[35] Z. Zhang, W. Wong, and J. Wu, "Ubiquitous human upper-limb motion estimation using wearable sensors," *Information Technology in Biomedicine, IEEE Transactions on*, vol. 15, no. 4, pp. 513–521, 2011.

[36] Z. Zhang, X. Meng, and J. Wu, "Quaternion-based kalman filter with vector selection for accurate orientation tracking," *Instrumentation and Measurement, IEEE Trans. on*, vol. 61, no. 10, pp. 2817–2824, 2012.

[37] BTSBioengineering. [Online]. Available: http://www.btsbioengineering.com/

Zhi-Qiang Zhang received the B.E. degree in computer science and technology from School of Electrical Information and Engineering, Tianjian University, China, in 2005, and the Ph.D. degree from the Sensor Network and Application Research Center, Graduate University, Chinese Academy of Sciences, Beijing, China, in 2010.

He is currently a Research Associate with the Hamlyn Centre for Robotic Surgery, Imperial College, London. His research interests include Body Sensor Network, Information Fusion, Machine Learning and Targets Tracking.

Guang-Zhong Yang (S'90-M'91-SM'08-F'11) is Director and Co-founder of the Hamlyn Centre for Robotic Surgery, Deputy Chairman of the Institute of Global Health Innovation, Imperial College London, UK. He also holds a number of key academic positions at Imperial: he is Director and Founder of the Royal Society/Wolfson Medical Image Computing Laboratory, co-founder of the Wolfson Surgical Technology Laboratory, Chairman of the Centre for Pervasive Sensing.

Dr Yang's main research interests are in medical imaging, sensing and robotics. In imaging, he is credited for a number of novel MR phase contrast velocity imaging and computational modelling techniques that have transformed in vivo blood flow quantification and visualization. These include the development of locally focused imaging combined with real-time navigator echoes for resolving respiratory motion for high-resolution coronary-angiography, as well as MR dynamic flow pressure mapping for which he received the ISMRM I. I Rabi Award. He pioneered the concept of perceptual docking for robotic control, which represents a paradigm shift of learning and knowledge acquisition of motor and perceptual/cognitive behaviour for robotics, as well as the field of Body Sensor Network (BSN) for providing personalized wireless monitoring platforms that are pervasive, intelligent, and context-aware.

The Hamlyn Centre directed by Prof Yang has been established for developing safe, effective and accessible imaging, sensing and robotics technologies that can reshape the future of healthcare for both developing and developed countries. Focusing on technological innovation but with a strong emphasis on clinical translation and direct patient benefit with a global impact, the centre is at the forefront of research in imaging, sensing and robotics for addressing global health challenges associated with demographic, environment, social and economic changes. The Centre plays an active role in international collaboration and outreach activities, as well as in the training of surgeons and engineers in medical imaging, sensing and robotics, thereby facilitating a fully integrated clinical approach.

Dr Yang is a Distinguished Lecturer for IEEE Engineering in Medicine and Biology Society. He is a Fellow of the Royal Academy of Engineering (RAEng), Fellow of IEEE, The Institution of Engineering and Technology (IET), The American Institute for Medical and Biological Engineering (AIMBE), The International Academy of Medical and biological Engineering (IAMBE), Society of Medical Imaging and Computer Assisted Intervention (MICCAI), City and Guilds of London and a recipient of the Royal Society Research Merit Award and The Times Eureka 'Top 100' in British Science.